0022-3565/09/3302-423–429$20.00
THE JOURNAL OF PHARMACOLOGY AND EXPERIMENTAL THERAPEUTICS
JPET 330:423–429, 2009

Vol. 330, No. 2
153551/3492469
Printed in U.S.A.

Dynamic Assessment of Mitoxantrone Resistance and Modulation of Multidrug Resistance by Valspodar (PSC833) in Multidrug Resistance Human Cancer Cells

Fei Shen, Barbara J. Bailey, Shaoyou Chu, Aimee K. Bence, Xinjian Xue, Priscilla Erickson, Ahmad R. Safa, William T. Beck, and Leonard C. Erickson

Indiana University Simon Cancer Center, Department of Pharmacology and Toxicology (F.S., B.J.B., A.K.B., X.X., P.E., A.R.S., L.C.E.), and Department of Cellular and Integrative Physiology (S.C.), Indiana University School of Medicine, Indianapolis, Indiana; and Department of Biopharmaceutical Sciences, University of Illinois at Chicago, Chicago, Illinois (W.T.B.)

Received March 16, 2009; accepted May 6, 2009

ABSTRACT

P-glycoprotein (Pgp), a member of the ATP-binding cassette transporter family, is one of the major causes for multidrug resistance (MDR). We report using confocal microscopy to study the roles of Pgp in mediating the efflux of the anticancer agent mitoxantrone and the reversal of MDR by the specific Pgp inhibitor valspodar (PSC833). The net uptake and efflux of mitoxantrone and the effect of PSC833 were quantified and compared in Pgp-expressing human cancer MDA-MB-435 (MDR) cells and in parental wild-type cells. The MDR cells, transduced with the human Pgp-encoding gene MDR1 construct, were approximately 8-fold more resistant to mitoxantrone than the wild-type cells. Mitoxantrone accumulation in the MDR cells was 3-fold lower than that in the wild-type cells. The net uptake of mitoxantrone in the nuclei and cytoplasm of MDR cells was only 58 and 67% of that in the same intracellular compartment of the wild-type cells. Pretreatment with PSC833 increased the accumulation of mitoxantrone in the MDR cells to 85% of that in the wild-type cells. In living animals, the accumulation of mitoxantrone in MDA-MB-435mdr xenograft tumors was 61% of that in the wild-type tumors. Administration of PSC833 to animals before mitoxantrone treatment increased the accumulation of mitoxantrone in the MDR tumors to 94% of that in the wild-type tumors. These studies have added direct in vitro and in vivo visual information on how Pgp processes anticancer compounds and how Pgp inhibitors modulate MDR in resistant cancer cells.

The use of anticancer agents in appropriate combinations has led to major improvements in the treatment of malignant tumors. Despite such successes, multidrug resistance (MDR) to various anticancer drugs due to an increased ability of cancer cells to extrude a variety of structurally and functionally unrelated cytotoxic compounds frequently occurs and is a major obstacle in clinical cancer treatment (Skatrud, 2002). Advances in elucidating the molecular basis of the MDR phenotype indicate that expressions of ATP-dependent transporters, including P-glycoprotein (Pgp) (ABCB1), are frequent causes of MDR (Ambudkar et al., 2003, 2006; Leslie et al., 2005). Cells transfected with the human MDR1 gene, which encodes Pgp, showed more resistance to anticancer drugs than parental wild-type cells (Gottesman and Pastan, 1993). The fact that these transfected cells have reduced intracellular drug accumulation and compromised effectiveness of anticancer drugs is believed to be due to the action of Pgp in mediating the efflux of cytotoxic drugs out of the cells and decreasing the net uptake of these agents into the cells. The correlation of Pgp overexpression in tumor tissues with decreased survival and poor prognosis has been reported clinically in some human cancers (van den Heuvel-Eibrink et al., 2000; Pakos and Ioannidis, 2003).

Mitoxantrone (Von Hoff et al., 1980), a Pgp substrate, is a synthetic anthracenedione that has been used in the clinical treatment of various cancers (Powles, 1997; Harris and Reese, 2001; Rigacci et al., 2003). The anticancer mechanisms of mitoxantrone are believed to be related to its capacity to bind DNA and inhibit DNA topoisomerase II in the nuclear compartment of the cells. In addition, the action of its metabolites in the intracellular cytosolic compartment may also contribute to the antineoplastic activities of mitoxantrone (Vibet et al., 2007). Decreased intracellular accumulation of mitoxantrone has been observed previously in Pgp-overexpressing cancer cells (Fukushima et al., 2000).

This work was supported by the National Institutes of Health National Cancer Institute [Grant CA9683901].
Article, publication date, and citation information can be found at http://jpet.aspetjournals.org.
doi:10.1124/jpet.109.153551.

ABBREVIATIONS: MDR, multidrug resistance; Pgp, P-glycoprotein; ABC, ATP-binding cassette transporter; PSC833, valspodar; wt, wild type.

Pgp is a target for anticancer chemotherapy modulation because of its molecular mechanisms in causing MDR. Inhibition of Pgp to sensitize cancer cells to chemotherapy has been widely studied. To date, three generations of Pgp inhibitors have been tested preclinically and clinically (Shukla et al., 2008). Valspodar (PSC833) (Gavériaux et al., 1991) is one of the second generation Pgp modulators, which reverses MDR by specifically binding to Pgp in the cell membrane. The antitumor efficacy of the combination of PSC833 and Pgp substrate anticancer drugs in animal studies has been reported by other investigators. The combination yielded greater reduction of tumor size and longer life span than the individual anticancer compound in animals bearing MDR tumors (Boesch et al., 1991). It was reported that the combination of PSC833 and doxorubicin significantly decreased the size of mice xenograft MDR breast tumors (Lopes de Menezes et al., 2003) and increased the life span of the mice carrying MDR leukemia by more than 80% (Watanabe et al., 1995). Coadministration of PSC833 and paclitaxel reduced mice glioblastoma volume by 90%, whereas paclitaxel itself did not affect the tumor volume. Furthermore, clinically PSC833 has shown the capacity to modulate MDR activities in acute myeloid leukemia, multiple myeloma, and ovarian cancer in phase I/II clinical trials (Advani et al., 1999; Bates et al., 2001; Carlson et al., 2006). However, like clinical trials of other Pgp inhibitors, the treatment with PSC833 only produced limited improvements in clinical outcome (Sikic, 1999). New effective Pgp modulators need to be developed.

Despite its limited clinical impact, PSC833 has been used in preclinical and clinical studies for developing new inhibitors and new clinical treatment regimens as well (Bates et al., 2001). In the current report, confocal microscopy was used to directly visualize and dynamically assess the intracellular drug accumulation and efflux process in Pgp expressing cancer cells. The in vitro and in vivo effects of Pgp on the intracellular accumulation and efflux of mitoxantrone and the effects of PSC833 on reversing MDR in these cells were evaluated. These studies have provided new information on direct visualization in real time of how MDR cells take up and efflux anticancer agents and how inhibitors modulate drug accumulation in cancer cells.

Materials and Methods

Reagents, Cell Lines, and Animals. Mitoxantrone was purchased from Sigma-Aldrich (St. Louis, MO). A stock solution was made by dissolving mitoxantrone in saline. PSC833 was a gift to W.T.B. from Dalia Cohen (Novartis Pharmaceuticals, Florham Park, NJ). Stock solutions were made by dissolving PSC833 in dimethyl sulfoxide for in vitro study and in a vehicle of sterile water/95% ethanol (7:3) for animal injections for in vivo study (Shen et al., 2008). Wild-type MDA-MB-435 (MDA-MB-435wt) human cancer cells and the MDA-MB-435 cells retrovirally transduced with the MDR1 gene to express Pgp (MDA-MB-435mdr, MDR cells) were obtained from Dr. George Sledge (Indiana University, Indianapolis, IN). The origin of MDA-MB-435 cells has been described previously (Shen et al., 2008).

Animal studies were carried out with protocols approved by the Animal Care and Use Committee of Indiana University. Female nude/nude mice, 6 to 8 weeks of age, were injected subcutaneously with human MDA-MB-435 cancer cells. Each mouse was injected with 15 to 20 $\times$ 10^6 MDA-MB-435wt cells in one flank and with 15 to 20 $\times$ 10^6 MDA-MB-435mdr cells in the other flank. The injection produced a palpable tumor within 3 to 4 weeks. Confocal image studies were then conducted on tumors in the mice.

Pgp Expression, Resistance to Mitoxantrone, and the Resistance Reversal by PSC833. Pgp expression was determined by Western blot assay. Cell lysates used for the analysis were prepared from crude cell membranes as described previously (Shen et al., 2008). Protein concentration in the cell lysates was determined with the Bradford assay (Bradford, 1976), and equal amounts of proteins were loaded on gels. Cell lysates were separated by SDS-polyacrylamide gel electrophoresis and transferred to a polyvinylidene difluoride membrane. The blot was then probed with the primary antibody C219 (dilution 1:1000) (ID Labs Inc., London, ON, Canada), followed by reaction with horseradish peroxidase-conjugated secondary antibody. The signal was detected using enhanced chemiluminescence and exposure of X-ray film.

Colony formation assays were used to evaluate the resistance of MDA-MB-435 cells to mitoxantrone and the reversal of the resistance by PSC833 (Shen et al., 2008). Cells were seeded in flasks and incubated under standard conditions overnight. Each group of three flasks of cells was treated with a different dose of mitoxantrone for 1 h. To assess the reversal of MDR by PSC833, the cells were pretreated with PSC833 30 min before mitoxantrone exposure. The cells were then washed, harvested, counted, and seeded into triplicate culture dishes. Colonies were fixed and visually counted after 14 days.

Mitoxantrone Intracellular Accumulation and Effects of PSC833. MDA-MB-435 cells were seeded on coverslips in 12-well plates and allowed to grow overnight. On the following day, cells were washed with phosphate-buffered saline, incubated with or without 3 mg/ml PSC833 for 30 min before being treated with 5 μM mitoxantrone for 2 h, and then examined using confocal microscopy.

Dynamic Assessment of Mitoxantrone Net Uptake, Efflux, and Effects of PSC833 in MDA-MB-435 Cells. MDA-MB-435 cells were seeded on coverslips overnight. The coverslips were mounted in microscope chambers. They were placed on the microscope stage and perfused sequentially with mitoxantrone-free medium for 6 min, medium with 5 μM mitoxantrone for 2 h (uptake perfusion), and then mitoxantrone-free medium again for 1 h (efflux perfusion). Serial images at 2-min intervals were collected and analyzed. To study the effect of PSC833 on the time course of mitoxantrone accumulation and efflux, MDA-MB-435 cells grown on coverslips were pre-exposed to 3 mg/ml PSC833 for 30 min before being mounted in microscope chambers for perfusion as described above.

Mitoxantrone Accumulation and Effects of PSC833 in Xenograft Tumors in Living Mice. Living nude mice bearing subcutaneous MDA-MB-435wt and MDA-MB-435mdr tumor xenografts in opposite flanks were injected with or without 50 mg/kg PSC833 intraperitoneally 1 h before receiving intravenous injection of 12.5 mg/kg mitoxantrone. Confocal tumor images were taken 2 h after the mice had received mitoxantrone. To obtain the images, the mice were anesthetized and a small skin incision was made to expose the tumor xenografts. The mice were placed on the microscope stage connected to a water circulator set to 37°C.

Confocal Microscopy and Image Analysis. Images were collected using an LSM510 NLO confocal microscope with a C-Apo 40$\times$ water immersion lens (Carl Zeiss, Jena, Germany). Mitoxantrone fluorescence was excited with an argon laser at 514 nm, and the emission was collected through a 530 nm long-pass filter. The same confocal settings (excitation, laser power, detector gain, and pinhole size) were used to image the wild-type and the MDR cells in vitro and the wild-type and MDR xenograft tumors in vivo. Post-data acquisition image analysis was performed using MetaMorph software (Molecular Devices, Sunnyvale, CA). Cell images were analyzed as mean mitoxantrone fluorescent intensity per pixel in a circular 314-pixel region of the nucleus or cytoplasm of the same cell (approximately 60 μm^2). Multiple fields containing at least 15 cells/field were imaged in each experiment. The tumor images were analyzed as mean mitoxantrone fluorescent intensity per pixel in a circular 785-pixel region

of the tumor. Three fields of each tumor were randomly picked for image analysis. Results were obtained from analyzing images from three to five experiments.

Statistics. All data are expressed as mean ± S.E. from three or more experiments and statistically evaluated by Student's t test. Differences were considered significant when $p < 0.05$.

Results

Pgp Expression, Resistance to Mitoxantrone, and the Resistance Reversal by PSC833. Pgp expression in MDA-MB-435 cells was demonstrated with Western blotting analysis. As shown previously by us (Shen et al., 2008), the monoclonal antibody C219 specifically detects a 180-kDa Pgp. A modest level of Pgp expression and no Pgp expression were observed in MDA-MB-435mdr and MDA-MB-435wt cells, respectively, compared with the vinblastine-selected $SKOV_3$ cells used as the positive control in this analysis (Shen et al., 2008).

The IC_{50} value of mitoxantrone in MDA-MB-435wt cells and MDA-MB-435mdr cells was 0.2 ± 0.03 μM (mean ± S.E.) and 1.6 ± 0.13 μM, respectively (Table 1). These results indicate that MDA-MB-435mdr cells were 8-fold more resistant to mitoxantrone than MDA-MB-435wt cells. Pretreatment with PSC833 decreased the IC_{50} value of mitoxantrone in MDA-MB-435mdr cells to 0.4 ± 0.02 μM (Table 1) in MDR cells and almost completely reversed the resistance of MDR cells to mitoxantrone. The pretreatment with PSC833 had no significant effect on the IC_{50} value of mitoxantrone in MDA-MB-435wt type cells.

Mitoxantrone Intracellular Accumulation and Effects of PSC833. Confocal cell images showed that mitoxantrone-associated fluorescence occurred in the nuclei and cytoplasm of MDA-MB-435wt cells. The fluorescence of mitoxantrone in MDA-MB-435mdr cells was weak and approximately 3-fold lower than that in the MDA-MB-435wt cells. Pretreatment of the MDR cells with PSC833 increased the fluorescent intensity in MDR cells to 85% of that in the wild-type cells (Fig. 1). The intracellular localization of mitoxantrone fluorescence in PSC833-pretreated MDR cells was the same as that in the wild-type cells. PSC833 had no significant effects on the intracellular distribution or accumulation of doxorubicin in the wild-type cells (data not shown).

Dynamic Assessment of Mitoxantrone Net Uptake, Efflux, and Effects of PSC833 in the Cytoplasm and Nuclei of MDA-MB-435 Cells. Sequential confocal cell images were used to assess and compare the real-time net uptake and efflux of mitoxantrone in the nuclei and cytoplasm of MDA-MB-435wt and MDA-MB-435mdr cells with or without pretreatment with PSC833. Compared with that in the same intracellular compartment of the wild-type cells, decreased accumulation of mitoxantrone in the nuclei (Fig. 2A) and cytoplasm (Fig. 2B) of the MDR cells was observed. In the uptake stage, the accumulation of mitoxantrone in both wild-type and MDR cells showed the same pattern. Mitoxantrone entered cellular nuclei and cytoplasm of the wild-type cells in two phases: little or no accumulation in the initial phase for approximately 25 min and a steady increase in mitoxantrone accumulation in a later phase. However, compared with that in the wild-type cells, the initial phase in the MDR cells was longer and slower. At the end of the 2-h mitoxantrone uptake perfusion, drug accumulation in the nuclei and cytoplasm of MDR cells was only 58 and 67% of that in the same intracellular compartment of the wild-type cells (Fig. 2C).

Mitoxantrone efflux occurred immediately in the MDR and wild-type cells after removal of mitoxantrone from the perfusates. The perfusion almost immediately brought mitoxantrone accumulation in the nuclei and cytoplasm of MDR cells to the baseline. The nuclei and cytoplasm of MDR cells lost 80% of the normalized intracellular mitoxantrone accumulation at the end of the perfusion phase. Meanwhile, only less than a 10% loss of normalized mitoxantrone accumulation was observed in the nuclei and cytoplasm of wild-type cells in the same perfusion study (Fig. 2D).

Pretreatment of MDA-MB-435mdr cells with the Pgp inhibitor PSC833 increased mitoxantrone net uptake and decreased drug efflux in the cells. At the end of the 2-h uptake perfusion, mitoxantrone accumulation in the nuclei of the pretreated MDR cells increased approximately 65% compared with that in the nonpretreated MDR cells (Fig. 2C). The same magnitude increase of mitoxantrone accumulation was also observed in the cytoplasm of pretreated MDR cells. The pretreatment increased the retention of mitoxantrone in the MDR cells to almost the same level as that in the wild-type cells at the end of efflux perfusion (Fig. 2D).

Mitoxantrone Accumulation and Effects of Pgp Inhibitors in Xenograft Tumors in Living Mice. Confocal tumor images were used to evaluate mitoxantrone accumulation and the effect of PSC833 on the accumulation in MDA-MB-435 xenograft tumors in vivo. Images of the MDA-MB-435wt xenograft tumors demonstrated similar intracellular mitoxantrone localization in vivo as that observed in vitro and showed mitoxantrone localized in both nuclei and cytoplasm of the cells. However, images of MDR xenograft tumors in vivo showed that mitoxantrone mainly localized in the nuclei area (Fig. 3). Tumor image analysis demonstrated significant differences of mitoxantrone fluorescent intensity in the MDR and wild-type tumors (Table 2) ($p < 0.05$). Mitoxantrone fluorescent intensity in the MDR tumors was only

TABLE 1
Cytotoxicity of mitoxantrone and modulation of drug resistance by PSC833 in human MDA-MB-435 cancer cells

Pretreatment	MDA-MB-435 Cell Type	IC_{50} of Mitoxantrone	RF[a]	FS[b]
		μM		
None	wt	0.2 ± 0.03	1.0	1.0
	MDR	1.6 ± 0.13	8.0*	1.0
PSC833 (3 mg/ml)	wt	0.2 ± 0.04	1.0	1.0
	MDR	0.4 ± 0.02	2.0	4.0*

* $p < 0.05$, statistically significant difference in drug resistance.
[a] Resistance factor: IC_{50} of mitoxantrone in MDR cells divided by IC_{50} of same drug in the wt cells.
[b] -Fold sensitization: IC_{50} of mitoxantrone in wt or MDR cells divided by that in the same cells pretreated with PSC833.

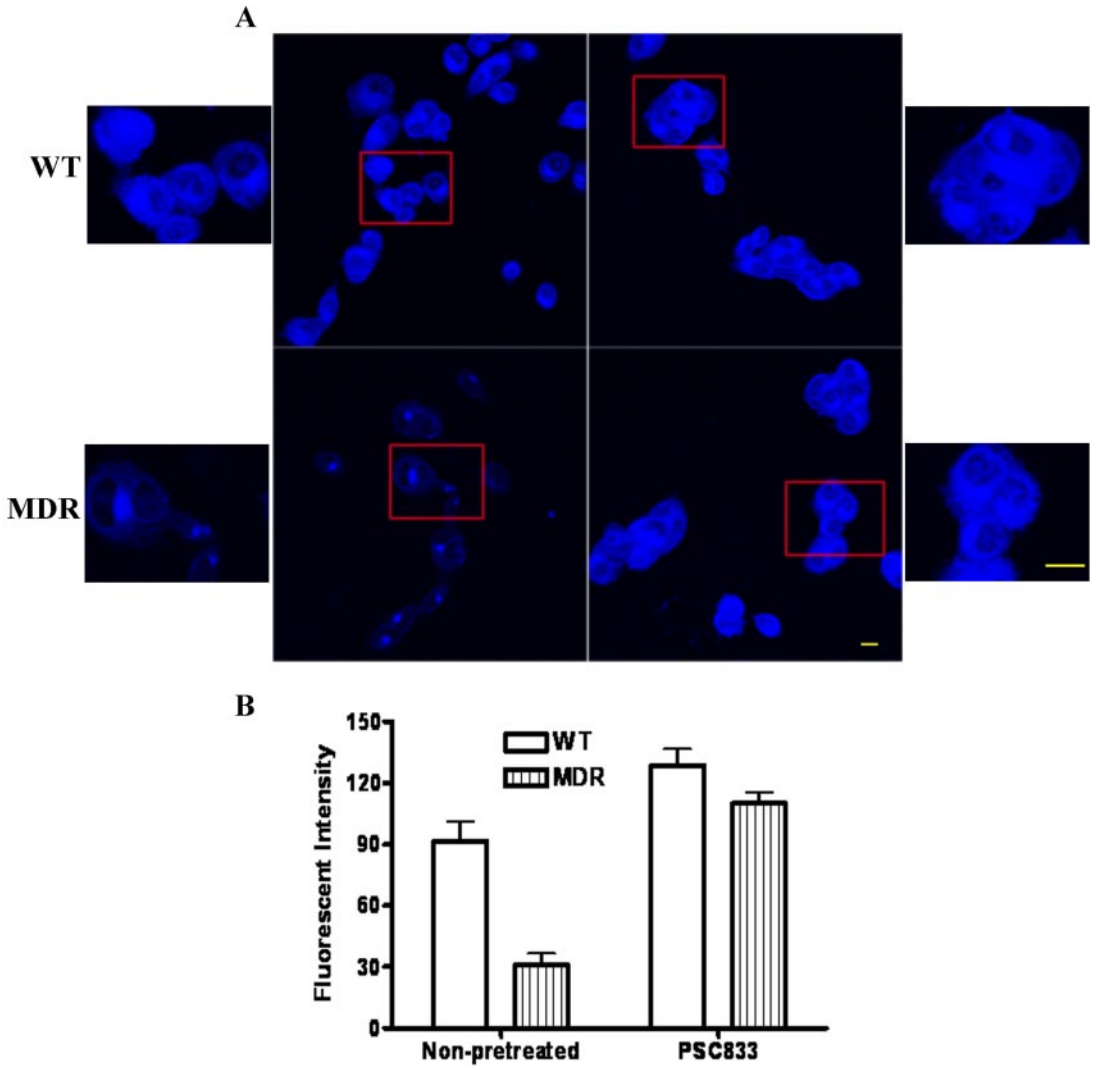

Fig. 1. Mitoxantrone accumulation in MDA-MB-435 cells pretreated or nonpretreated with Pgp inhibitor PSC833. A, confocal cell images (scale bar, 10 μm; smaller images are a higher magnification; scale bar, 10 μm) of the boxed areas in the adjacent figures. B, histograms indicating drug accumulation. Values are mean ± S.E. *, $p < 0.05$, significant difference of fluorescent intensity of mitoxantrone in the wild-type and in the MDR cells.

61% of that in the wild-type tumors. Preadministration of PSC833 to mice increased mitoxantrone fluorescent intensity in MDR tumor to 94% of that in the wild-type tumors. A similar intracellular localization pattern of mitoxantrone was observed in MDR and the wild-type tumors in the pretreated mice. Mitoxantrone accumulation in MDR tumors in the pretreated mice increased 36% compared with that in the nonpretreated animals.

Discussion

The innate fluorescence of mitoxantrone was used in this study to elucidate the role of Pgp in causing multidrug resistance in cancer cells. Although mitoxantrone is also known as a substrate of another ABC transporter breast cancer resistant protein (ABCG2) (Litman et al., 2000), the focus of this study was only on Pgp.

Compared with the wild-type cells, MDA-MB-435mdr cells were 8-fold more resistant to mitoxantrone. However, the fluorescent intensity of mitoxantrone in the MDR cells was only 3-fold lower than that of the wild-type cells. The discrepancy between the magnitude of resistance to mitoxantrone and the reduction of mitoxantrone accumulation in the MDR cells may be due, at least in part, to mitoxantrone exhibiting low levels of fluorescence (Bell, 1988), which may have affected the accuracy of its fluorescent quantification in this study. The study suggests that the fluorescent intensity of mitoxantrone is not linearly proportional to the intracellular accumulation of mitoxantrone; however, the results indicate a trend in correlation exists between the potency of mitoxantrone (cytotoxicity) and the intracellular accumulation of the compound (fluorescent intensity).

The localization of mitoxantrone in both cellular nuclei and cytoplasm has been also reported by other investigators (Fox and Smith, 1995; Feofanov et al., 1997). We reported previously that the intracellular distribution pattern of doxorubicin in MDA-MB-435wt cells was mainly in the cellular nuclei. Doxorubicin and mitoxantrone both exert their cytotoxicity by binding DNA and inhibiting nuclei acid synthesis. However, the apparent cytoplasmic localization of mitoxantrone may indicate that some cytoplasmic targets, including mitochondria and/or lysosome as reported by other investigators, are also involved in its cytotoxic mechanism (Smith et al.,

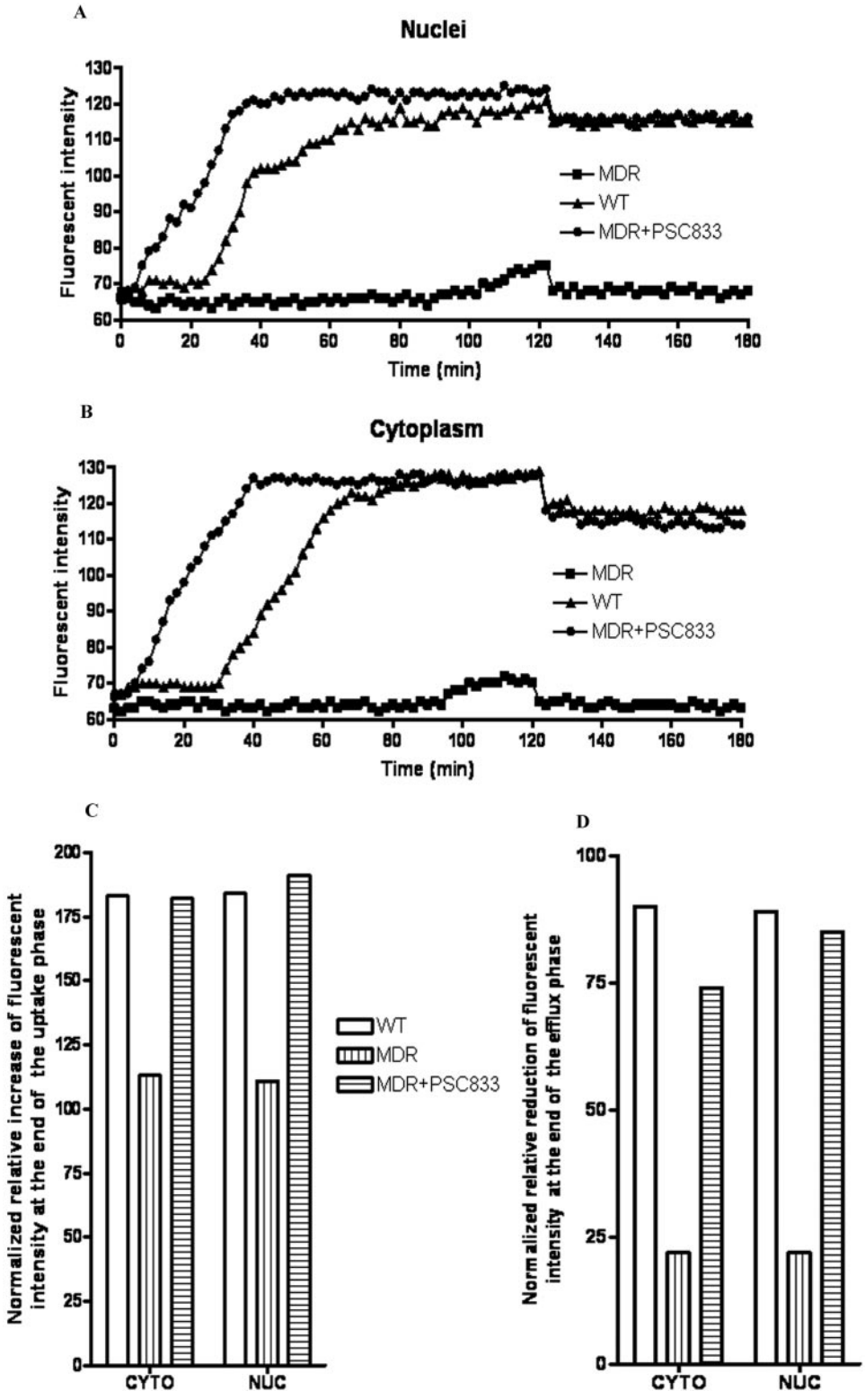

Fig. 2. Net uptake and efflux of mitoxantrone in MDA-MB-435 cells in the nuclei of the cells (A) and in the cytoplasm of the cells (B). Accumulation of mitoxantrone in the nuclei and cytoplasm of MDA-MB-435 cells at the end of uptake perfusion (C) and at the end of efflux perfusion (D). Fluorescent intensity (accumulation) of mitoxantrone in intracellular nuclei and cytoplasm at the end of uptake and efflux perfusion was calculated relative to that in the same cellular compartment at the baseline level and at the end of uptake perfusion, respectively.

1992). The possibility that mitoxantrone and its metabolites target both cellular nuclei and cytoplasm may explain our observation that the IC_{50} value of mitoxantrone in MDA-MB-435 human cancer cells was 3-fold lower than that of doxorubicin (Cutts et al., 2003). The same magnitude increase of mitoxantrone uptake in the nuclei and cytoplasm of the wild-type cells (Fig. 2) further supports that mitoxantrone targets both cellular nuclei and cytoplasm. The two phases observed in the uptake stage of mitoxantrone could be explained, at least in part, by the accumulation of mitoxantrone being required to reach a threshold level for the confocal microscope to detect intracellular mitoxantrone. These results on the intracellular localization of mitoxantrone suggest that confocal microscopy is a useful technique in studying the cellular targets of various therapeutic agents.

The significantly lower mitoxantrone fluorescent intensity

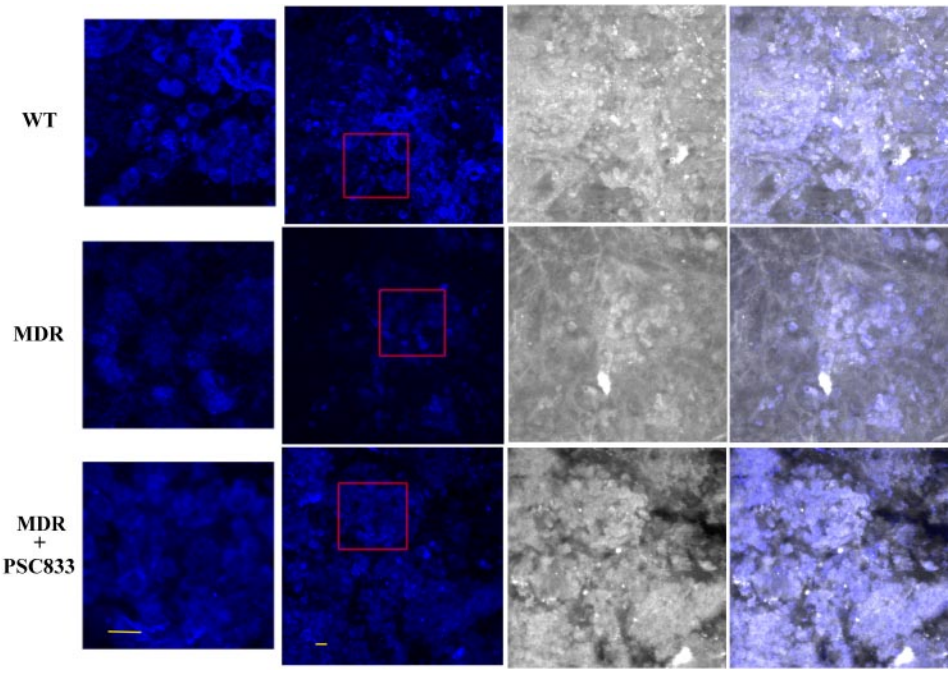

Fig. 3. In vivo confocal images of mitoxantrone accumulation in MDA-MB-435wt tumor xenograft (top) and drug-resistant MDA-MB-435mdr tumor xenograft (middle), and MDA-MB-435mdr tumor xenograft pretreated with PSC833 (bottom). Confocal images (left), reflecting images (middle), overlays of confocal and reflecting images (right). Scale bar, 10 μm. Smaller images are a higher magnification (scale bar, 10 μm) of the boxed areas in the adjacent figures.

TABLE 2
Mitoxantrone accumulation in MDA-MB-435 xenograft tumors
Fluorescent intensity values are mean ± S.E.

Pretreated with	Tumor Type	Fluorescent Intensity	% of wt Tumors	% of Nonpretreated wt Tumors	% of Nonpretreated MDR Tumors
None	wt	91.1 ± 27.3	100		
	MDR	55.6 ± 6.4	61*		100
PSC833	wt	81.2 ± 12.6		100	
	MDR	75.8 ± 5.3		94	136**

* $p < 0.05$, statistically significant difference of fluorescent intensity of mitoxantrone in MDA-MB-435wt tumors and MDA-MB-435mdr tumors.
** $p < 0.05$, statistically significant difference of fluorescent intensity of mitoxantrone in nonpretreated and pretreated MDA-MB-435mdr tumors.

in vivo in the MDR xenograft tumors compared with that in the wild-type xenograft tumors was consistent with the lower accumulation of mitoxantrone in vitro observed in the MDR cells compared with that in the wild-type cells. It is not fully understood why mitoxantrone localized only in the nuclei of MDR tumor cells in vivo. One explanation might be that the affinity of mitoxantrone to cellular nuclei DNA was stronger than that to some cytoplasmic structure(s), which made the drug distribution only in the nuclei of MDR tumor cells when the cells had a low accumulation level of the compound. Compared with that in the wild-type tumor cells, the cytoplasm of MDR tumor cells had a markedly lower accumulation of mitoxantrone, which may explain our observation that mitoxantrone accumulation in the MDR tumors was only 61% of that in the wild-type tumors and supports the idea that a cytoplasmic structure(s) is involved in the anticancer mechanism of mitoxantrone in the wild-type tumors. PSC833, a specific Pgp inhibitor, not only increased the fluorescent intensity of mitoxantrone and reversed the resistance to mitoxantrone in MDR cells in vitro but also restored the distribution of mitoxantrone in the cytoplasm of MDR tumor cells in vivo, indicating that intracellular accumulation levels of mitoxantrone in vivo affect the intracellular localization of the drug.

This article provides direct information on the capacity of the ABC transporter Pgp to mediate the efflux of substrate anticancer drug mitoxantrone in real time and decrease intracellular drug accumulation in vitro and in vivo. This study suggests confocal microscopy is a useful technique in evaluating MDR transporters in vitro and in vivo and therefore is helpful toward the future development of MDR inhibitors.

References

Advani R, Saba HI, Tallman MS, Rowe JM, Wiernik PH, Ramek J, Dugan K, Lum B, Villena J, Davis E, Paietta E, Litchman M, Sikic BI, and Greenberg PL (1999) Treatment of refractory and relapsed acute myelogenous leukemia with combination chemotherapy plus the multidrug resistance modulator PSC 833 (valspodar). *Blood* **93:**787–795.

Ambudkar SV, Kim IW, and Sauna ZE (2006) The power of the pump: mechanisms of action of P-glycoprotein (ABCB1). *Eur J Pharm Sci* **27:**392–400.

Ambudkar SV, Kimchi-Sarfaty C, Sauna ZE, and Gottesman MM (2003) P-glycoprotein: from genomics to mechanism. *Oncogene* **22:**7468–7485.

Bates S, Kang M, Meadows B, Bakke S, Choyke P, Merino M, Goldspiel B, Chico I, Smith T, Chen C, et al. (2001) A phase I study of infusional vinblastine in combination with the P-glycoprotein antagonist PSC 833 (valspodar). *Cancer* **92:** 1577–1590.

Bell DH (1988) Characterization of the fluorescence of the antitumor agent, mitoxantrone. *Biochim Biophys Acta* **949:**132–137.

Boesch D, Gavériaux C, Jachez B, Pourtier-Manzanedo A, Bollinger P, and Loor F (1991) In vivo circumvention of P-glycoprotein-mediated multidrug resistance of tumor cells with SDZ PSC 833. *Cancer Res* **51:**4226–4233.

Bradford MM (1976) A rapid and sensitive method for the quantitation of microgram quantities of protein utilizing the principle of protein-dye binding. *Anal Biochem* **72:**248–254.

Carlson RW, O'Neill AM, Goldstein LJ, Sikic BI, Abramson N, Stewart JA, Davidson NE, and Wood WC (2006) A pilot phase II trial of valspodar modulation of multidrug resistance to paclitaxel in the treatment of metastatic carcinoma of the breast (E1195): a trial of the Eastern Cooperative Oncology Group. *Cancer Invest* **24:**677–681.

Cutts SM, Swift LP, Rephaeli A, Nudelman A, and Phillips DR (2003) Sequence specificity of adriamycin-DNA adducts in human tumor cells. *Mol Cancer Ther* **2:**661–670.

Feofanov A, Sharonov S, Fleury F, Kudelina I, and Nabiev I (1997) Quantitative confocal spectral imaging analysis of mitoxantrone within living K562 cells: intra-

cellular accumulation and distribution of monomers, aggregates, naphtoquinoxaline metabolite, and drug-target complexes. *Biophys J* **73:**3328–3336.
Fox ME and Smith PJ (1995) Subcellular localisation of the antitumour drug mitoxantrone and the induction of DNA damage in resistant and sensitive human colon carcinoma cells. *Cancer Chemother Pharmacol* **35:**403–410.
Fukushima T, Yamashita T, Takemura H, Suto H, Kishi S, Urasaki Y, and Ueda T (2000) Effect of PSC 833 on the cytotoxicity and pharmacodynamics of mitoxantrone in multidrug-resistant K562 cells. *Leuk Res* **24:**249–254.
Gavériaux C, Boesch D, Jachez B, Bollinger P, Payne T, and Loor F (1991) SDZ PSC833, a non-immunosuppressive cyclosporin analog, is a very potent multidrug-resistance modifier. *J Cell Pharmacol* **2:**10.
Gottesman MM and Pastan I (1993) Biochemistry of multidrug resistance mediated by the multidrug transporter. *Annu Rev Biochem* **62:**385–427.
Harris KA and Reese DM (2001) Treatment options in hormone-refractory prostate cancer: current and future approaches. *Drugs* **61:**2177–2192.
Leslie EM, Deeley RG, and Cole SPC (2005) Multidrug resistance proteins: role of P-glycoprotein, MRP1, MRP2, and BCRP (ABCG2) in tissue defense. *Toxicol Appl Pharmacol* **204:**216–237.
Litman T, Brangi M, Hudson E, Fetsch P, Abati A, Ross DD, Miyake K, Resau JH, and Bates SE (2000) The multidrug-resistant phenotype associated with overexpression of the new ABC half-transporter, *MXR (ABCG2). J Cell Sci* **113:**2011–2021.
Lopes de Menezes DE, Hu Y, and Mayer LD (2003) Combined treatment of Bcl-2 antisense oligodeoxynucleotides (G3139), p-glycoprotein inhibitor (PSC833), and sterically stabilized liposomal doxorubicin suppresses growth of drug-resistant growth of drug-resistant breast cancer in severely combined immunodeficient mice. *J Exp Ther Oncol* **3:**72–82.
Pakos EE and Ioannidis JPA (2003) The association of P-glycoprotein with response to chemotherapy and clinical outcome in patients with osteosarcoma. A meta-analysis. *Cancer* **98:**581–589.
Powles TJ (1997) Evolving clinical strategies: innovative approaches to the use of mitoxantrone—introduction. *Eur J Cancer Care (Engl)* **6 (4 Suppl):**1–3.
Rigacci L, Carpaneto A, Alterini R, Carrai V, Bernardi F, Bellesi G, Longo G, Bosi A, and Rossi Ferrini P (2003) Treatment of large cell lymphoma in elderly patients with a mitoxantrone, cyclophosphamide, etoposide, and prednisone regimen: long-term follow-up results. *Cancer* **97:**97–104.
Shen F, Chu S, Bence AK, Bailey B, Xue X, Erickson PA, Montrose MH, Beck WT, and Erickson LC (2008) Quantitation of doxorubicin uptake, efflux, and modulation of multidrug resistance (MDR) in MDR human cancer cells. *J Pharmacol Exp Ther* **324:**95–102.
Shukla S, Wu CP, and Ambudkar SV (2008) Development of inhibitors of ATP-binding cassette drug transporters: present status and challenges. *Expert Opin Drug Metab Toxicol* **4:**205–223.
Sikic BI (1999) New approaches in cancer treatment. *Ann Oncol* **10 (Suppl 6):**149–153.
Skatrud PL (2002) The impact of multiple drug resistance (MDR) proteins on chemotherapy and drug discovery. *Prog Drug Res* **58:**99–131.
Smith PJ, Sykes HR, Fox ME, and Furlong IJ (1992) Subcellular distribution of the anticancer drug mitoxantrone in human and drug-resistant murine cells analyzed by flow cytometry and confocal microscopy and its relationship to the induction of DNA damage. *Cancer Res* **52:**4000–4008.
van den Heuvel-Eibrink MM, Sonneveld P, and Pieters R (2000) The prognostic significance of membrane transport-associated multidrug resistance (MDR) proteins in leukemia. *Int J Clin Pharmacol Ther* **38:**94–110.
Vibet S, Mahéo K, Goré J, Dubois P, Bougnoux P, and Chourpa I (2007) Differential subcellular distribution of mitoxantrone in relation to chemosensitization in two human breast cancer cell lines. *Drug Metab Dispos* **35:**822–828.
Von Hoff DD, Pollard E, Kuhn J, Murray E, and Coltman CA Jr (1980) Phase I clinical investigation of 1,4-dihydroxy-5,8-bis (((2-[(2-hydroxyethyl)amino]ethyl) amino))-9,10-anthracenedione dihydrochloride (NSC 301739), a new anthracenedione. *Cancer Res* **40:**1516–1518.
Watanabe T, Tsuge H, Oh-Hara T, Naito M, and Tsuruo T (1995) Comparative study on reversal efficacy of SDZ PSC 833, cyclosporin A and verapamil on multidrug resistance in vitro and in vivo. *Acta Oncol* **34:**235–241.

Address correspondence to: Dr. Fei Shen, Indiana University Simon Cancer Center, Cancer Research Institute, R3-C222, 1044 West Walnut St., Indianapolis, IN 46202. E-mail: fshen@iupui.edu